Chemical Genetics Identifies Small-Molecule Modulators of Neuritogenesis Involving Neuregulin-1/ErbB4 Signaling

Letian Kuai,[†] Xiang Wang,[‡] Jon M. Madison,[†] Stuart L. Schreiber,[§] Edward M. Scolnick,[†] and Stephen J. Haggarty*[,†,⊥]

[†]Stanley Center for Psychiatric Research, Broad Institute of Harvard and MIT, 7 Cambridge Center, Cambridge, Massachusetts 02142, [‡]Department of Chemistry and Biochemistry, University of Colorado, 215 UCB, Boulder, Colorado 80309, [§]Chemical Biology Program, Broad Institute of Harvard and MIT, 7 Cambridge Center, Cambridge, Massachusetts 02142, and [⊥]Center for Human Genetic Research, Massachusetts General Hospital, Department of Neurology, Harvard Medical School, 185 Cambridge Street, Boston, Massachusetts 02114

Abstract

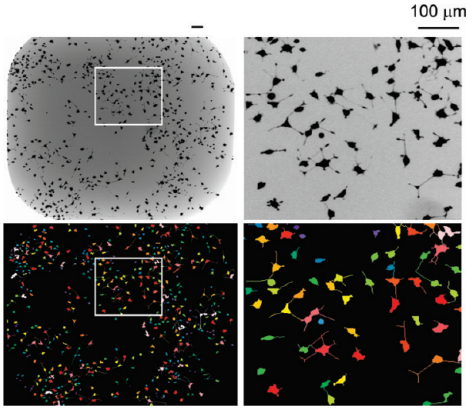

Genetic findings have suggested that neuregulin-1 (Nrg1) and its receptor v-erb-a erythroblastic leukemia viral oncogene homologue 4 (ErbB4) may play a role in neuropsychiatric diseases. However, the downstream signaling events and relevant phenotypic consequences of altered Nrg1 signaling in the nervous system remain poorly understood. To identify small molecules for probing Nrg1−ErbB4 signaling, a PC12-cell model was developed and used to perform a live-cell, image-based screen of the effects of small molecules on Nrg1-induced neuritogenesis. By comparison of the resulting phenotypic data to that of a similar screening performed with nerve growth factor (NGF), this multidimensional screen identified compounds that directly inhibit Nrg1−ErbB4 signaling, such as the 4-anilinoquinazoline Iressa (gefitinib), as well as compounds that potentiate Nrg1−ErbB4 signaling, such as the indolocarbazole K-252a. These findings provide new insights into the regulation of Nrg1−ErbB4 signaling events and demonstrate the feasibility of using such a multidimensional, chemical-genetic approach for discovering probes of pathways implicated in neuropsychiatric diseases.

Keywords: Neuregulin, ErbB4, automated imaging, neuritogenesis, quinazoline, indolocarbazole

Chemical genetics aims to discover small molecules that can be used as probes to alter protein function. This approach provides an important path both to decipher the molecular circuitry that regulates complex biological phenotypes and to potentially identify new targets for therapeutic intervention. There has been a dramatic increase in the application of chemical genetics to a variety of biological systems and disease contexts (*1*). However, to date this approach has not been widely used to dissect the function of candidate disease genes and pathways implicated in neuropsychiatric disorders.

Genetic analysis of several neuropsychiatric disorders has led to the identification of several potential risk genes and has opened up the possibility of testing their functional significance. In the case of schizophrenia (OMIM 181500), a highly heritable and devastating neuropsychiatric disorder that affects between 0.5% and 1.0% of the world's population, the genes encoding neuregulin-1 (Nrg1) (*2*−*4*) and its 180-kDa transmembrane tyrosine kinase receptor ErbB4 (v-erb-a erythroblastic leukemia viral oncogene homologue 4) of the epidermal growth factor receptor (EGFR) family have been identified as susceptibility genes (*5*−*11*). Nrg1 and ErbB4 have been implicated in a variety of neuronal development processes, including neuritogenesis (the formation of extended processes that become axons and dendrites), neuronal migration, myelination and synapse formation, as well as multiple forms of synaptic plasticity (*12*, *13*), many of which have been implicated in the pathogenesis of schizophrenia as well as other psychiatric diseases. While Nrg1 and ErbB4 are attractive susceptibility genes, functional variation in these genes has yet to link clearly Nrg1−ErbB4 signaling to the pathogenesis of schizophrenia. In fact, contradictory data exist that suggest decreases or increases in Nrg1−Erb4 signaling may account for disease pathogenesis. For instance, decreased Nrg1

Received Date: December 29, 2009
Accepted Date: January 7, 2010
Published on Web Date: January 28, 2010

DOI: 10.1021/cn900046a | *ACS Chem. Neurosci.* (2010), *1*, 325–342

signaling has been proposed to contribute to altered brain development, neurotransmission, and cortical function, while an alternative gain-of-function hypothesis suggests increased levels of Nrg1 and ErbB4 (*14*) and high Nrg1−ErbB4 signaling (*15*) exist in the prefrontal cortex of schizophrenia patients. Despite this intriguing progress, clear functional evidence connecting these risk genes to schizophrenia still does not exist (*13*).

The difficulty of establishing clear functional association between Nrg1−Erb4 signaling and psychiatric disease is partially due to the diversity of Nrg1 isoforms and family members and the diversity of ErbB family of transmembrane receptors. The Nrg1 gene encodes multiple proteins containing an EGF-like domain that binds to the extracellular domain of ErbB family receptors, either in a paracrine or in a juxtacrine signaling manner, and causes receptor dimerization (*16*). ErbB receptor dimerization stimulates the intrinsic tyrosine kinase activity of these receptors leading to autophosphorylation and subsequent recruitment of a variety of signaling molecules. In addition, the ErbB4 gene is known to undergo alternative splicing to encode either a metalloprotease cleavable (JM-a) or cleavage-resistant (JM-b) extracellular domain and a cytoplasmic domain (Cyt-1), a phosphotidylinositol-3 kinase (PI3K) binding site, or Cyt-2 (*17*−*19*). Among the four members of the ErbB family, ErbB3 and ErbB4 are known to have Nrg1-binding ability. The former lacks a functional kinase domain and is believed to be a kinase-dead ErbB isoform. ErbB3 is known to play an active role in regulating the function of other ErbB family members. EGFR (ErbB1) and ErbB2 do not bind Nrg1, but these receptors can be activated by heterodimerizing with ErbB3 and ErbB4 upon Nrg1 induction (*13*, *20*). In addition to Nrg1 and EGF, the ErbB family receptors can also respond to other growth factors, such as transforming growth factor alpha (TGFα) and HB-EGF (*21*). Thus, dissecting the complexity of Nrg1−ErbB4 poses a great challenge especially since no specific ErbB4 inhibitor is currently available.

Besides understanding how genetic variation influences nervous system function, a major focus of the field of neurobiology is to understand the molecular machinery and mechanisms that enable neuronal networks to be generated and remodeled throughout development and in response to neural activity. Neuritogenesis, the initial stage of neuronal differentiation, involves the generation of processes termed neurites that emerge from the cell body of postmitotic cells. These processes extend steadily until one (the future axon) starts growing more rapidly, inducing morphological polarization. In primary neurons, both in cell culture and *in vivo*, the extension of neurites leads to the establishment of polarity in which one process becomes an axon and the remaining processes become dendrites, and then they eventually establish synapses. Besides initiating differentiation, neuritogenesis plays an important role in the initiation of neuronal migration and patterning that gives rise to the intricate networks of neuronal connections in the adult brain. Consistent with the fundamentally important role of neuritogenesis, a growing number of neuropsychiatric disease risk genes, such as Nrg1 and DISC1, have been shown to alter neurite formation (*22*). These findings suggest that by using neurite outgrowth as a phenotype, it may be possible to develop small-molecule probes that can be used to target and discover new properties of the underlying signaling networks that are integral to the etiology and pathophysiology of severe mental illnesses. To initiate systematic efforts to test this notion, we describe herein the development and characterization of a model PC12 cell system expressing ErbB4 and the results of a phenotype-based screen for differential modulators of Nrg1- versus NGF-induced neuritogenesis.

Results and Discussion

To develop a cellular model that would enable chemical-genetic characterization of Nrg1−ErbB4 signaling and discovery of new small-molecule probes, we chose the neuroendocrine cell line PC12 (*23*), derived from a rat pheochromocytoma, as a model neuronal system for several reasons. First, PC12 cells do not naturally express ErbB4 but are known to express EGFR (ErbB1), ErbB2, and ErbB3, so this would allow us to express exogenous genetically altered ErbB4 receptors. Second, PC12 cells engineered to express human ErbB4 have been reported to differentiate and undergo neuritogenesis upon treatment with recombinant Nrg1 (*24*), which we reasoned could provide a phenotype that could be quantified using automated microscopy and image analysis. Finally, NGF-induced differentiation has been extensively studied in PC12 cells, and much is known about the downstream signaling pathways, which we reasoned would assist in comparing the selectivity of any compounds that we identify.

To create a system for chemical-genetic study, we prepared a stable PC12 cell line that coexpresses green fluorescent protein (GFP) and the human ErbB4 isoform JMa-Cyt2 and a control cell line PC12-GFP that stably expresses GFP but lacks ErbB4. The PC12-ErbB4-GFP cells were examined by fluorescence imaging for the effects of NGF and Nrg1 on neurite outgrowth. As expected, both the PC12-ErbB4-GFP and the PC12-GFP cell lines exhibited the characteristic morphological changes indicative of neuronal differentiation involving neurite outgrowth when treated with NGF (Figure 1A). Under low magnification ($< 10\times$), the distribution of coexpressed GFP is uniform throughout the

DOI: 10.1021/cn900046a | *ACS Chem. Neurosci.* (2010), *1*, 325–342

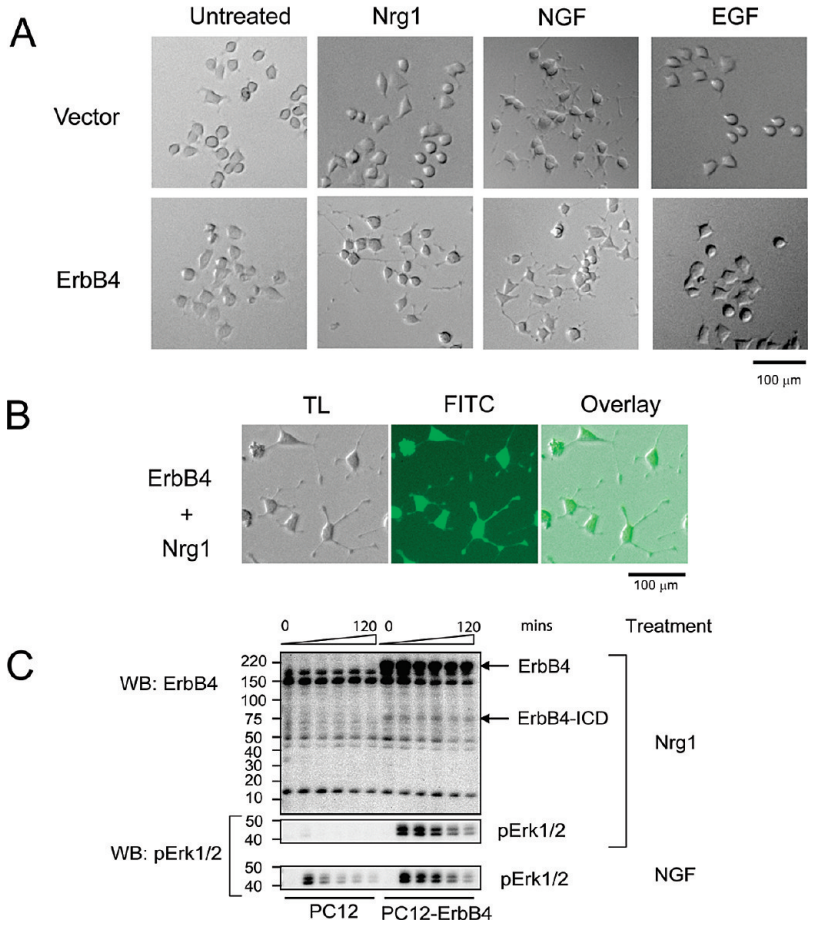

Figure 1. Nrg1 induces neurite outgrowth and Erk1/2 phosphorylation in PC12-ErbB4-GFP cells. (A) PC12-GFP (vector) and PC12-ErbB4-GFP (ErbB4) cells were seeded in a 96-well plate at 1200 cells/well and incubated at 5% CO_2, 37 °C, for 12 h and then were treated with Nrg1 (20 ng/mL) or NGF (20 ng/mL) or left untreated, as indicated, for 3 days. Transmitted light cell images were taken using a 10× objective. (B) Green fluorescence image (FITC channel) of Nrg1-treated PC12-ErbB4-GFP cell was overlaid with transmitted light image (TL channel). (C) PC12-GFP (vector) and PC12-ErbB4-GFP (ErbB4) cells were treated with Nrg1 (20 ng/mL) or NGF (20 ng/mL) for the indicated times. Whole cell extracts were subjected to immunoblotting with antibodies against ErbB4 or phospho-pErk, respectively, as indicated.

cell body and neurite projections, and the fluorescent image reliably represents the whole cell body and attached processes (Figure 1B). Nrg1 stimulation of PC12-ErbB4-GFP cells, but not PC12-GFP, for 2 days resulted in significant neurite outgrowth similar to the effects of NGF. This result indicated that although PC12 cells express ErbB3, which can also bind to Nrg1 and heterodimerize with other ErbB family members, the presence of the ErbB4 receptor is necessary for Nrg1 signaling to stimulate neuritogenesis. In addition, EGF treatment failed to stimulate neurite outgrowth in both cell lines (Figure 1A), suggesting that although EGFR-activation might also activate other ErbB receptors via heterodimerization, it is not capable of triggering neuritogenesis in the presence or absence of ErbB4.

ErbB4 is known to activate downstream effectors of neurotrophic factor pathways such as mitogen-activated protein kinase (MAPK). To verify that PC12-ErbB4-GFP cells activate MAPK pathway components in response to Nrg1, we examined the ability of NGF and Nrg1 treatment to activate of the MAPK pathway as measured by phosphorylation of extracellular signal-regulated kinase (Erk1/2). In both the PC12-GFP and PC12-ErbB4-GFP cell lines, NGF induced a rapid phosphorylation of Erk1/2, which peaked as early as 5 min after treatment. In contrast, Nrg1 induced a strong phosphorylation of Erk1/2 only in PC12-ErbB4-GFP cells (Figure 1C). In addition, it has been reported that Nrg1 increases the release of the intracellular domain of ErbB4, ErbB4-ICD, in neural precursor cells (*25*). However, we did not observe this effect in PC12 cells (Figure 1C). We also found that a γ-secretase inhibitor that is known to inhibit the cleavage of ErbB4 did not inhibit Nrg1-induced neurite outgrowth in PC12-ErbB4 cells (data not shown).

Automated Live-Cell Neurite Outgrowth Assay

Having validated that stimulation of PC12-ErbB4-GFP cells with Nrg1 could induce neuritogenesis, we sought next to determine whether the outgrowth

DOI: 10.1021/cn900046a | *ACS Chem. Neurosci.* (2010), *1*, 325–342

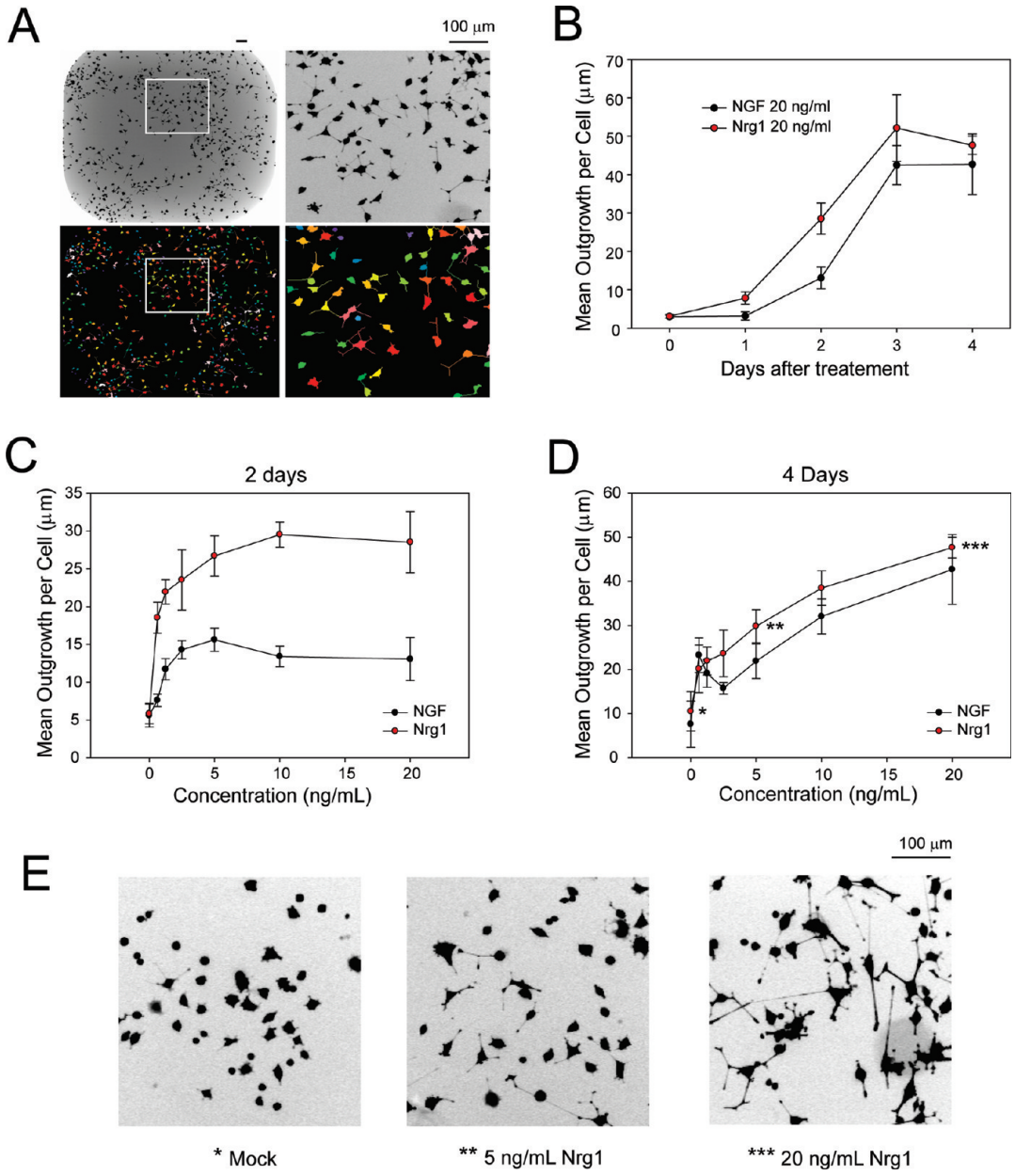

Figure 2. Nrg1- and NGF-induced neurite outgrowth is dose-dependent and quantitatively measurable. PC12-ErbB4-GFP cells were seeded in 384-well assay plates at 400 cells/well for 12 h and then left untreated or treated with Nrg1 or NGF at indicated concentrations. Fluorescent images of cells were acquired automatically every 24 h and analyzed. (A) Demonstration of a typical neurite detection result from the MetaXpress software. Upper panel shows the cell image acquired with a 4× objective; lower panel shows computer-generated mask of cell bodies and neurites. Mean neurite outgrowth per cell was determined after cell body and neurite detection. (B) Growth curve of neurites induced by Nrg1 and NGF at 20 ng/mL over a 4-day course. (C) Dose−response curve of Nrg1 and NGF determined at day 2. (D) Dose−response curve of Nrg1 and NGF determined at day 4. (E) Representative image of PC12-ErbB4-GFP treated without (mock) or with 5 and 20 ng/mL Nrg1 for 4 days. Error bar represents SEM, $n = 4$.

phenotype was suitable for use with automated imaging and image analysis. The expression of soluble GFP in PC12 cells allowed the use of automated microscopy to acquire fluorescent images for the quantitative analysis of cell number and morphological changes associated with neuronal differentiation over a developmental time course. To minimize cell clumping and intersection of neurites in 96- or 384-well plates for time periods of up to 4 days, we seeded cells at a low density of ~4000 cells/cm^2. Imaging with an ImageXpress 5000A automated microscope equipped with 4× objective enabled the acquisition of the entire well of a 384-well plate in one image with sufficient resolution to accurately detect and quantify various properties of neurites and cell bodies. A typical pixel map of the segmentation mask generated by the MetaXpress software is shown in Figure 2A.

DOI: 10.1021/cn900046a | ACS Chem. Neurosci. (2010), 1, 325–342

Cell bodies were identified as pixel blocks with minimum area of 200 μm^2 and maximum width of 40 μm, and the neurites were subsequently identified as line objects longer than 10 μm and connected to each cell body. The mean neurite length per cell for each well was quantified as a single parameter (see the Methods section for a more detailed description of imaging and analysis parameters), represented as "mean outgrowth per cell (μm)". We accounted for variation in cell density due to seeding or to the effect of antiproliferative compounds by quantifying neurite outgrowth on a per-cell basis. The use of automated image analysis methods enabled the accurate assessment of morphological properties of hundreds of cells per well without human bias of which cells to measure the properties.

We studied the robustness of our automated neurite detection by comparing the dose response of PC12-ErbB4-GFP cells to Nrg1 and NGF as a function of time with image acquisition every 24 h. Both NGF and Nrg1 stimulated a continuous increase in mean neurite length over a four- day time course. NGF-treated cells appeared to differentiate more slowly than Nrg1-treated cells in the first 24 h, but after four days, the mean length of neurites per cell in both treatments was similar (Figure 2B). This delayed response to NGF, but similar overall effect after four days, might be explained by an up regulation of the expression levels of the tyrosine kinase receptor TrkA (*26*) or a secondary receptor of NGF, such as $p75^{NTR}$ (*27*), which is known to potentiate the activity of TrkA through the formation of a high-affinity NGF receptor. The mean neurite length exhibited a strong correlation to the dose of Nrg1 or NGF added to the cells especially under concentrations of 10 ng/mL at day two (Figure 2C) and under 20 ng/mL at day four (Figure 2D). These data suggested that we could use automated microscopy to measure neurite length as a phenotype for screening.

ErbB4 Activation Is Sufficient for Nrg1-Dependent Neuritogenesis

Having established methods for quantitatively measuring Nrg1-induced neuritogenesis in PC12-ErbB4-GFP cells, before embarking on a screen for chemical modulators, we sought to better understand the signaling events associated with Nrg1−ErbB4 signaling to assist in the eventual downstream characterization of any probes that might be identified. Besides activating ErbB4 homodimers, Nrg1 can mediate the formation of ErbB dimers consisting of ErbB3 (*21*), as well as EGFR (*20*). Thus, although ErbB4 is required for Nrg1 to promote neurite outgrowth, since all ErbB family members are expressed in the PC12-ErbB4-GFP cells, it remained unclear whether the other ErbB receptors were also playing a role. To address specifically the contribution of other ErbB family members to Nrg1−ErbB4 dependent neurite outgrowth, we individually reduced the expression of ErbB1/EGFR, ErbB2, and ErbB3 with pools of small inhibitory RNAs (siRNAs). The efficacy and specificity of each ErbB receptor siRNA pool was verified by Western blotting (Figure 3A). The Nrg1-driven neurite outgrowth was diminished only when ErbB4 expression was reduced (Figure 3B,C), suggesting that ErbB1/EGFR, ErbB2, and ErbB3 do not contribute significantly to Nrg1-dependent neuritogenesis in PC12 cells and that ErbB4 is necessary for the observed effects of Nrg1 on neuritogenesis. These results are consistent with the observation that PC12 cells only extended neurites in response to Nrg1 when the ErbB4 receptor was expressed. Surprisingly, we observed that reducing ErbB3 expression enhanced Nrg1-induced neurite outgrowth, suggesting that ErbB3 inhibits some aspect of neuritogenesis in our PC12 cell system. While the molecular basis for this observation is not understood, it suggests that ErbB3, although lacking a functional kinase domain, may contribute to the signaling of kinase-active ErbB receptors as well as other proteins important for neuritogenesis (*28*).

Nrg1-Dependent Neuritogenesis Is Inhibited by MEK inhibitors but Not PI3K Inhibitors

To investigate the downstream components of Nrg1−ErbB4 signaling that triggers neuritogenesis, we specifically examined two key kinase cascades coupled to receptor tyrosine kinase signaling, MEK and PI3K pathways. The ERK kinase (MEK) has long been known to mediate NGF-induced PC12 differentiation (*29*). In our system, two specific MEK inhibitors, PD098059 and U0126, attenuated both NGF- and Nrg1-induced neurite outgrowth (Figure 3D,E). These results further validated that both Nrg1- and NGF-induced neuritogenesis are dependent on the Erk1/2 cascade. PI3K is another important component of many neurotrophic factor signal transduction pathways. Although we used the human ErbB4 isoform JMa-Cyt2, which lacks the PI3K binding domain, it has been demonstrated that all ErbB4 isoforms, including Cyt2 isoforms, associate with and activate PI3K (*30*). Consistent with this finding, we observed an up-regulation of phosphorylated Akt (Ser473), an indicator of PI3K activation, when cells were exposed to Nrg1 (data not shown). To determine whether both NGF- and NRG1-induced neuritogenesis requires PI3K signaling, PC12-ErbB4-GFP cells were treated with two structurally distinct PI3K inhibitors, LY294002 and wortmannin. Both of these PI3K inhibitors caused an inhibitory effect on NGF-induced neurite outgrowth as expected (*31*). In contrast, neither LY294002 nor wortmannin were capable of inhibiting Nrg1-induced neurite outgrowth at doses ranging from 0.1 to 10 μM (Figure 3B). Collectively, these results suggest that although both Nrg1 and NGF stimulate Erk1/2 and PI3K cascades, activation of

DOI: 10.1021/cn900046a | ACS Chem. Neurosci. (2010), 1, 325–342

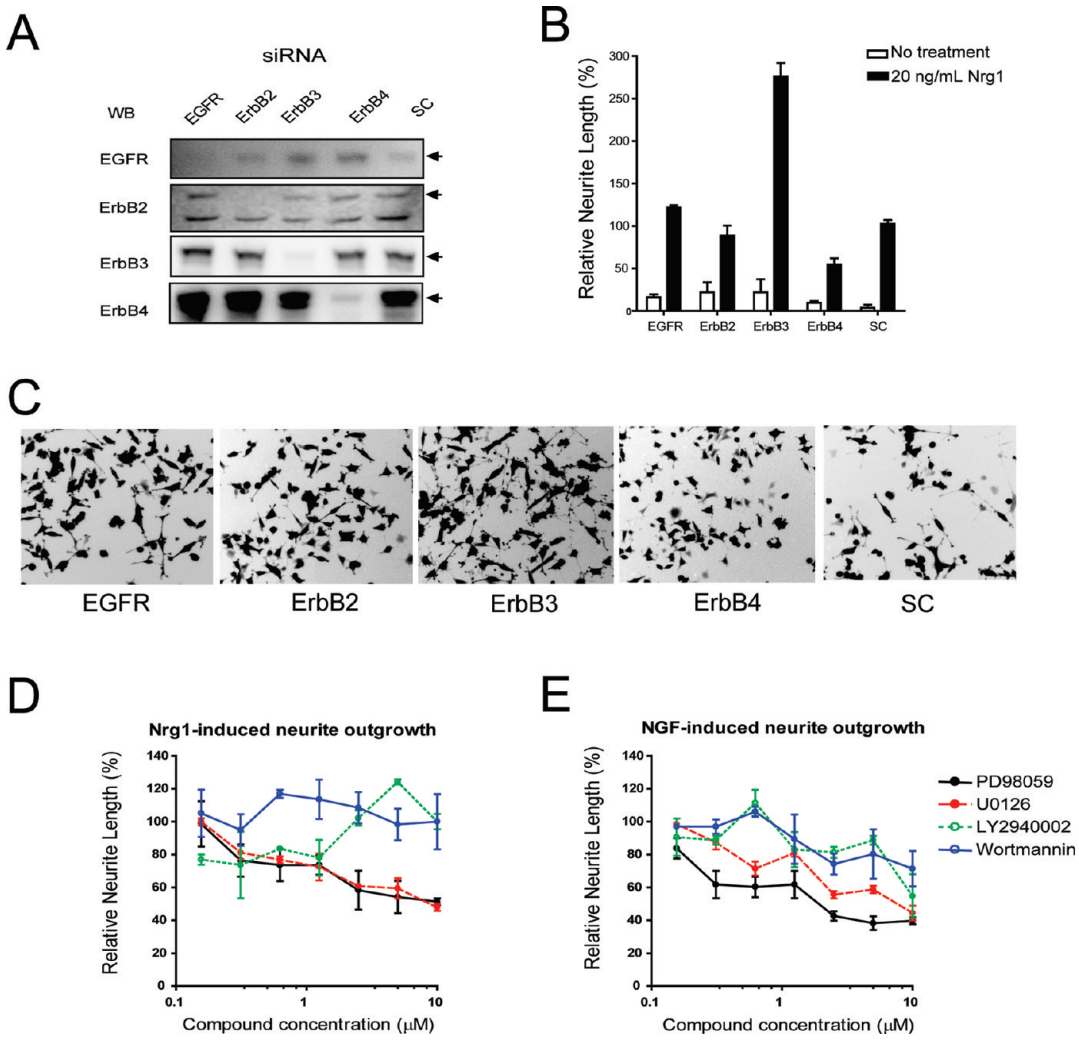

Figure 3. Nrg1-driven neurite outgrowth is ErbB4- and Erk1/2-dependent. PC12-ErbB4-GFP cells were seeded in a 96-well assay plate at 3000 cells/well for 12 h followed by transfection of siRNAs specific for EGFR, ErbB2, ErbB3, ErbB4, and scrambled (SC), as indicated, for 48 h. (A) The transfected cells were then induced with 20 ng/mL Nrg1 and imaged 48 h after the induction with 4× objectives. Representative cropped images are shown. (B) Whole cell extracts of the transfected cells were subjected to Western blotting with antibodies against EGFR, ErbB2, ErbB3, and ErbB4. Equal loading was measured using a nonspecific band recognized by ErbB2 antibody. (C) Nrg1-induced neurite outgrowth in panel A was analyzed with MetaXpress Neurite Outgrowth algorithm. Neurite outgrowth is presented relative to that in scrambled siRNA-transfected cells treated with 20 ng/mL Nrg1. PC12-ErbB4-GFP cells were seeded in a 384-well assay plate at 400 cells/well for 12 h and then treated with serially diluted PD98059, U0126, LY294002, and wortmannin for 30 min followed by treatment with 20 ng/mL Nrg1 and 20 ng/mL NGF. Fluorescent cell images were acquired with 4× objective after 48 h and analyzed with MetaXpress Neurite Outgrowth algorithm. Data is presented relative to that from cells treated with DMSO and then Nrg1 (D) or NGF (E). Error bar represents SEM, $n = 4$.

PI3K is not required for neuritogenesis induced by Nrg1 in our PC12 cellular system.

Discovery of Small-Molecule Probes of Nrg1-Induced Neuritogenesis

Having shown that our cellular model activated neuritogenesis in an Nrg1−ErbB4-dependent manner and retained the ability to respond to NGF, we next screened for small molecules that could specifically modulate Nrg1−ErbB4 signaling without affecting NGF-induced neuritogenesis. We initially tested 400 known bioactive small molecules at a single dose (~10 μM) for their ability to modulate neurite outgrowth induced by the addition of Nrg1 and NGF (see Supplementary Tables 1 and 2, Supporting Information, for the complete list of compounds tested and resulting high-content imaging data). A total of three 384-well plates (one DMSO control plate and two compound plates each containing 200 bioactives and 184 DMSO control wells) were screened (Figure 4A).

Cell morphological features measured from each image using MetaXpress software included (1) percent of cells with significant neurite growth, (2) number of cells, (3) total neurite outgrowth, (4) mean neurite outgrowth length per cell, (5) normalized mean neurite outgrowth per cell, (6) mean number of processes per cell, (7) mean branches per cell, and (8) mean cell body

DOI: 10.1021/cn900046a | ACS Chem. Neurosci. (2010), 1, 325–342

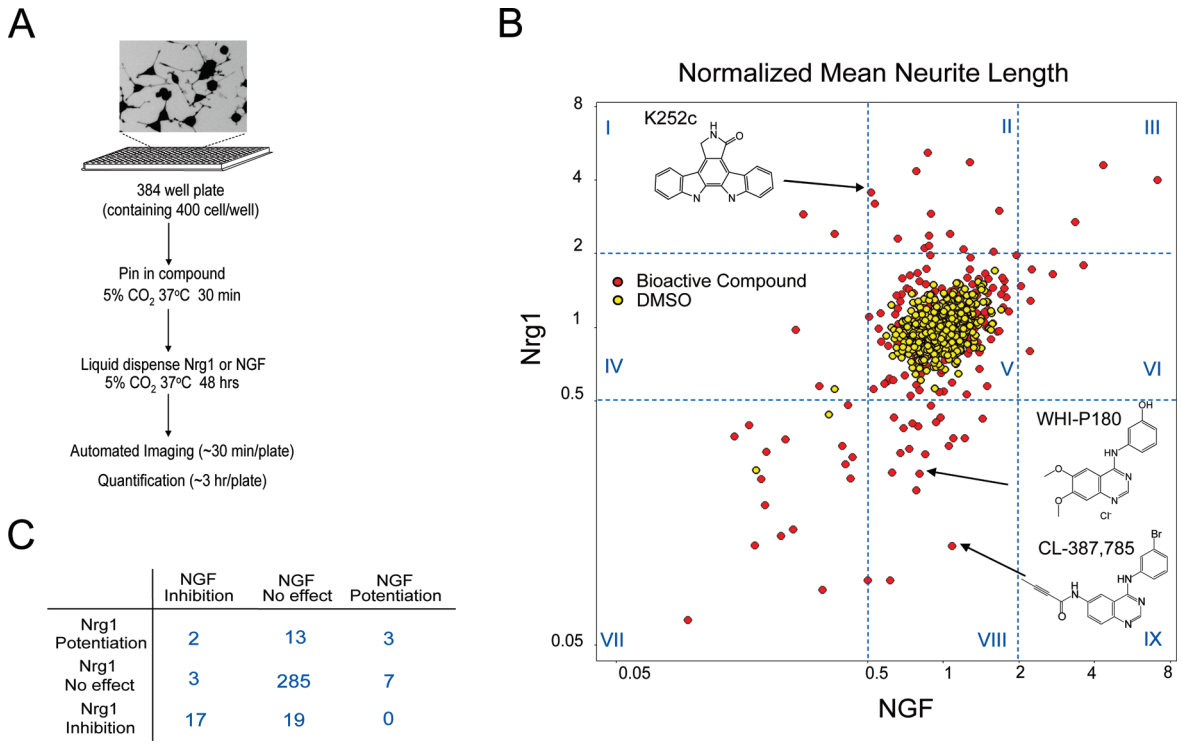

C

	NGF Inhibition	NGF No effect	NGF Potentiation
Nrg1 Potentiation	2	13	3
Nrg1 No effect	3	285	7
Nrg1 Inhibition	17	19	0

Figure 4. Image-based assay of 400 bioactive small molecules. (A) Summary of the overall HTS performed using the PC12-ErbB4-GFP cell line. Cells were seeded in 384-well assay plate at 400 cells/well and incubated for 12 h. Compounds were then pin-transferred into the wells 30 min before Nrg1 (20 ng/mL) and NGF (20 ng/mL) were introduced by automated-liquid dispensing to each well. Fluorescent images of each well were acquired and analyzed after 48 h incubation. (B) Overall categorization of the screening results into nine activity classes (I−IX). Boundaries were set at 2- and 0.5-fold of mean neurite outgrowth per cell of 752 DMSO control wells. Members of each class are described in more detail in Supplementary Tables 1 and 2, Supporting Information. (C) The effect of each compound (red circle) in the presence of either Nrg1 or NGF compared using the computed mean neurite outgrowth per cell. The 752 DMSO control wells are shown as yellow circles. Three compounds that lead to further characterization of the chemical space surrounding them in this study are marked by arrows.

area. Each feature is described in the Methods section in more detail, and the complete data set for Nrg1- and NGF-treated wells is provided in Supplementary Tables 1 and 2, respectively, in the Supporting Information. Supplementary Tables 3−10, Supporting Information, provide a global statistical analysis of the eight cellular features, an assessment of the degree to which the cellular feature is normally distributed, and the observed relationships of each feature to each other in the form of Pearson correlation coefficient. Based upon these global analyses, as shown in Supplementary Figure 3, Supporting Information, a graphical representation of the two-dimensional Pearson correlation map between the eight cellular features in the Nrg1 and NGF high-content imaging screens reveals that many of these cellular features are highly correlated across the 400 compound treatments and there existed differences in the global feature profiles between Nrg1 and NGF. However, we also noticed that there were potentially informative relationships among the cellular and neurite features. For instance, in the case of Nrg1-treated cells (see Supplementary Figure 4, Supporting Information), the mean neurite length feature was correlated with the percentage of cells with significant neurite outgrowth ($r = 0.93$) and the number of processes per cell ($r = 0.95$) but was more moderately correlated with the number of branches measured per cell ($r = 0.70$). In contrast, the mean neurite length per cell correlated less with cell body size ($r = 0.5$) suggesting that Nrg1-induced neuritogenesis can be separated from the control of soma size.

Since we found that the mean neurite length per cell feature was strongly positively correlated to the dose and duration of Nrg1 and NGF treatment (Figure 2), we chose this feature as a surrogate of Nrg1 and NGF signaling for use in image-based screening while recognizing that analysis of other features may lead to different types of modulators of Nrg1 signaling. With this feature, in our assay, the 752 DMSO control wells for each treatment exhibited consistent background levels of neurite outgrowth and changes in cell number (see Supplementary Tables 3 and 4, Supporting Information). The mean neurite length values from each set of DMSO control treatments was taken as the baseline value. For subsequent data visualization, the mean neurite length value in each well upon Nrg1 or NGF induction was normalized to the respective baseline value (Figure 4B). Within the library of 400 known

DOI: 10.1021/cn900046a | ACS Chem. Neurosci. (2010), 1, 325–342

bioactives, 51 compounds led to a significant reduction in cell number in either the Nrg1 or NGF treatment conditions as defined by a threshold of having less than 100 cells after two days of incubation. While these compounds may have additional phenotypes at lower concentrations, they were not considered further in the studies reported here. The remaining 349 compounds were categorized into nine classes based on their relative activities compared with the DMSO controls and their specificities toward Nrg1- and NGF-induced neurite outgrowth (Figure 4B) using a simple fold-change cutoff of 2-fold for molecules that potentiated neurite outgrowth and 0.5-fold for molecules that inhibited outgrowth. The numbers of bioactives in each category based upon this classification are summarized in Figure 4C.

Characterization of 4-Anilino-quinazoline-Based Inhibitors of Nrg1 Signaling

To identify specific inhibitors of Nrg1−ErbB4 signaling, we first focused our analysis on those compounds that inhibited Nrg1-induced neurite outgrowth but had no effect on NGF-induced neurite outgrowth. From our original screen, we noted that two 4-anilino-quinazoline-containing compounds, WHI-P180 and CL-387,785, satisfied our selection criteria (Figure 4C) and had no effect on the cell number, indicating that they did not alter cell proliferation over the two-day time course.

While both WHI-P180 and CL-387,785 were previously shown to inhibit EGFR (*32*, *33*), little was known about the ability of these two compounds to inhibit Nrg1 signaling. 4-Anilino-quinazoline-based compounds are known to reversibly and competitively bind to the ATP pocket of EGFR (*34*). To further explore the ability of 4-anilino-quinazoline-based compounds to inhibit Nrg1-signaling, we tested four commonly used small molecules of this structural class: AG1478, PD158780, Iressa (gefitinib), and Tarceva (erlotinib) (Figure 5A), along with nine additional 4-anilino-quinazolines also classified as EGFR inhibitors (Supplementary Figure 2, Supporting Information). Iressa and Tarceva are Food and Drug Administration (FDA)-approved drugs used for the treatment of non-small-cell lung cancer through a mechanism thought to involve the inhibition of the tyrosine kinase activity of EGFR and have been optimized for their pharmacological properties and safety in humans. All four 4-anilino-quinazolines inhibited Nrg1-induced outgrowth in a dose-dependent manner, while PD158780 appeared to have a lower potency (at ~2 μM) against Nrg1 stimulation and decrease the mean length of neurites induced by NGF at the same concentration. On the other hand, AG1478, Iressa, and Tarceva had no significant effect on NGF-induced neurite outgrowth but all inhibited Nrg1-induced neurite outgrowth with EC_{50}'s of ~500 nM (Figure 5B). The two irreversible EGFR inhibitors, CL-387,785 and PD168393, were both superior inhibitors of Nrg1-induced neurite outgrowth ($EC_{50} \approx 100$ nM), while PD168393 exhibited the strongest inhibition of NGF-induced neurite outgrowth as well (Supplementary Figure 2, Supporting Information). CP-724,714, reported to be an inhibitor ErbB2 selective over EGFR (*35*), was the weakest compound to inhibit Nrg1 ($EC_{50} \approx 4\,\mu$M) (Supplementary Figure 2, Supporting Information). Taken together, most of the 4-anilino-quinazoline-based compounds in this study inhibit Nrg1-induced neurite outgrowth with various efficacies and specificities over NGF-induced neurite outgrowth.

Inhibition of ErbB4 Activation by Nrg1 Signaling

While Iressa was originally developed to selectively target EGFR (*36*), our results described here suggest that Iressa also inhibits ErbB4-dependent neuritogenesis. To characterize the interaction between Iressa and ErbB4 in greater detail and to test whether Iressa inhibits the activation of ErbB4 by Nrg1, ErbB4 was immunoprecipitated from PC12-ErbB4-GFP cells after a short exposure to Nrg1 with or without Iressa treatment. The phosphorylation status of ErbB4, a measure of receptor activity, was examined using a phosphotyrosine specific antibody. Indeed, the phosphorylation of ErbB4 receptors induced by Nrg1 was inhibited when cells were treated with Iressa (2 μM), and the subsequent phosphorylation of the downstream Erk1/2 was also diminished. In contrast, Iressa did not affect NGF-induced activation of Erk1/2, thereby confirming the selectivity observed for the 4-anilino-quinazolines in the initial small-molecule screen (Figure 5C). In addition, when cells were treated with Nrg1 (20 ng/mL), the phosphorylation levels of ErbB4 and Erk1/2 were diminished by Iressa (0.2−5 μM) in a dose-dependent manner as determined by Western blotting with phospho-ErbB4 and phospho-Erk1/2 antibodies (Figure 5D,E), respectively. These results indicate that Iressa treatment inhibits ErbB4 receptor activation and its downstream signaling.

Cellular and Biochemical Characterization of Targets of Iressa Involved in Neuritogenesis

Although we demonstrated that ErbB4 activation is necessary and sufficient for Nrg1-induced neuritogenesis (Figure 1A) and that the activation of ErbB4 is inhibited by Iressa (Figure 5D,E), it remained possible that the inhibition is indirect through inhibition of trans-phosphorylation by other ErbB family members or other targets. Since ErbB3 lacks kinase activity, we ruled this ErbB receptor out as a direct target. It is also known that Iressa inhibits EGFR ($IC_{50} \approx 30$ nM) more potently than ErbB2 ($IC_{50} > 3.7\,\mu$M) (*36*). Furthermore, the selective ErbB2-inhibitor, CP-724,714, poorly inhibited Nrg1-induced neurite outgrowth (Supplementary Figure 2, Supporting Information), suggesting that

DOI: 10.1021/cn900046a | ACS Chem. Neurosci. (2010), 1, 325–342

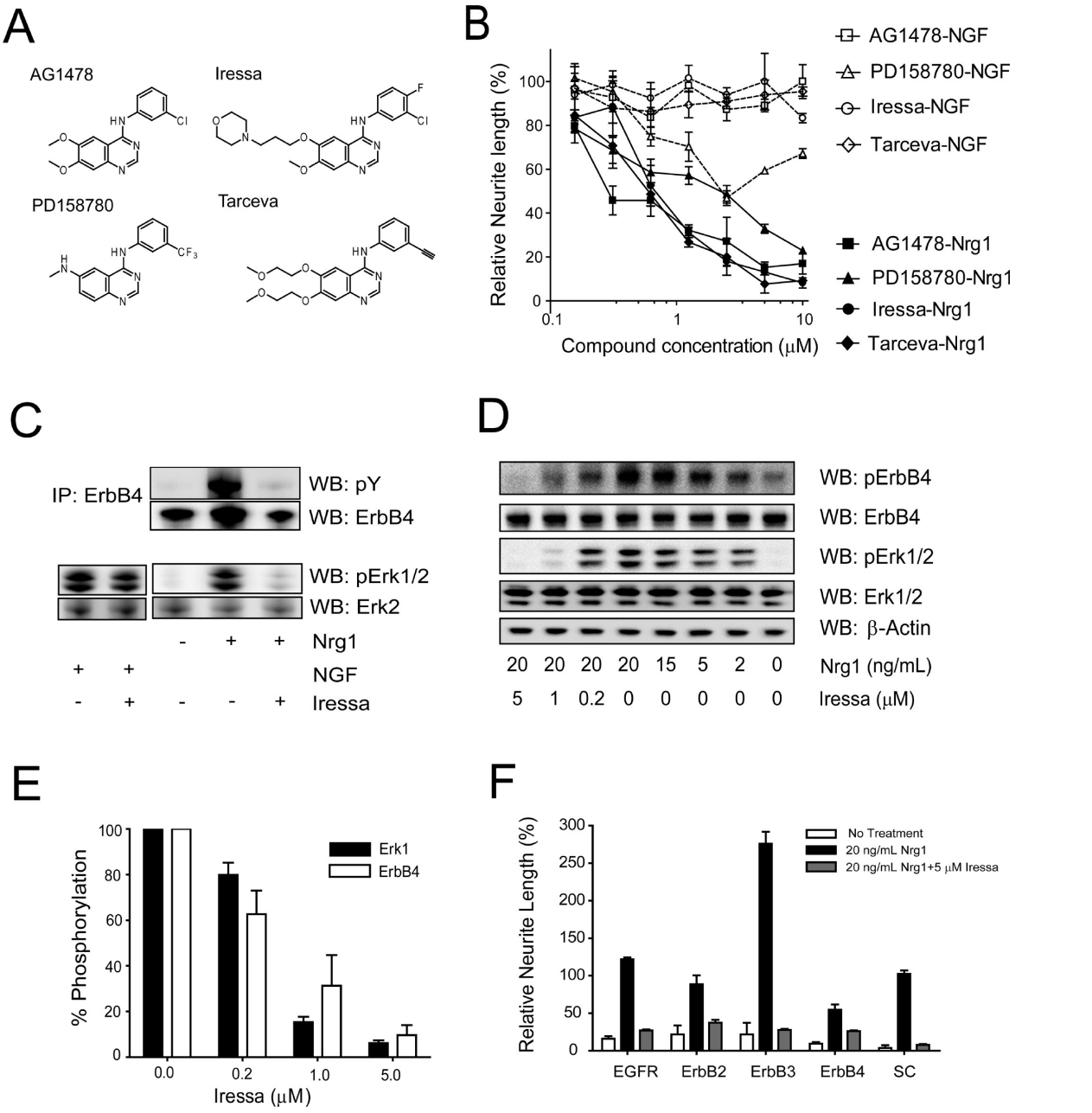

Figure 5. Characterization of 4-anilino-quinazolines that inhibit Nrg1-induced neurite outgrowth. (A) Structures of four representative 4-anilino-quinazolines, AG1478, PD158780, Iressa, and Tarceva. (B) PC12-ErbB4-GFP cells were pretreated with serially diluted 4-anilino-quinazolines for 30 min followed by 20 ng/mL of Nrg1 or NGF. Fluorescent images of cells were acquired after 2 days incubation and analyzed with MetaXpress Neurite Outgrowth algorithm. Neurite outgrowth is presented relative to that in cells treated with DMSO and then Nrg1 or NGF, respectively. (C) Cells were pretreated with Iressa (5 μM) or DMSO for 30 min followed by 20 ng/mL of Nrg1 or NGF and lysed after 5 min. Whole cell lysates were immunoprecipitated by anti-ErbB4 antibody followed by Western blotting with antibodies against phosphotyrosine and ErbB4. Phospho-Erk1/2 and total Erk2 levels were determined by direct Western blotting with whole cell lysates. (D) Cells were pretreated with various concentrations of Iressa or DMSO for 30 min followed by various concentrations of Nrg1 and lysed after 5 min. Levels of phospho-ErbB4, phospho-Erk1/2, total ErbB4, total Erk1/2, and β-actin were determined by Western blotting with specific antibodies. (E) Levels of phospho-ErbB4 and phospho-Erk1/2 were quantified and normalized to total ErbB4 and Erk1/2, respectively, and plotted against concentration of Iressa. (F) PC12-ErbB4-GFP cells were seeded in 96-well assay plate at 3000 cells/well for 12 h followed by transfection of siRNAs specific for EGFR, ErbB2, ErbB3, ErbB4, and scrambled (SC), as indicated, for 48 h. The transfected cells were then treated with 5 μM Iressa for 30 min followed by induction with 20 ng/mL Nrg1 for 48 h. Neurite outgrowth is presented relative to that from scrambled siRNA-transfected cells treated with 20 ng/mL Nrg1. Error bar represents SEM, $n = 4$.

inhibiting ErbB2 is not critical. Thus, we focused our efforts on determining whether the inhibition of ErbB4 is due to an indirect inhibition of EGFR.

To determine whether Iressa acts through ErbB4 to inhibit neurite outgrowth, to complement the chemical treatments described above, we used RNAi-mediated

DOI: 10.1021/cn900046a | ACS Chem. Neurosci. (2010), 1, 325–342

silencing to reduce the levels of ErbB family members and then treated with Iressa. Iressa was found to still effectively diminish neurite outgrowth in cells where expression of EGFR, ErbB2, or ErbB3 was reduced by siRNAs (Figure 5F), suggesting that none of these three ErbB family members are required for Iressa's effects on Nrg1 signaling and that their loss-of-function does not potentiate the effect of Iressa. Of note, even though ErbB3 silencing potentiated the effects of Nrg1, the enhanced neurite outgrowth observed upon ErbB3 knock down was still blocked by Iressa treatment. This result suggests either that the neuritogenesis signaling caused by ErbB3 depletion is transduced through ErbB4 signaling itself or that Iressa causes a dominant inhibition of an alternative signaling pathway that mediates the alterations of neuritogenesis caused by loss of ErbB3.

Based on the cellular results described above, we used three other lines of investigation to further test the hypothesis that the 4-anilino-quinazolines identified here act as direct inhibitors of ErbB4 kinase activity. First, to demonstrate that Iressa interacts with full-length ErbB4 receptor in a physiologically relevant setting, we created a new chemical tool, "iTrap", consisting of Iressa immobilized on an agarose solid support and performed affinity chromatography (Figure 6A). iTrap was able to affinity-capture full-length ErbB4 and ErbB4-ICD (intracellular domain containing the kinase domain) in PC12-ErbB4-GFP but not the parental PC12-GFP cells lacking ErbB4 expression (Figure 6B). Most importantly, the levels of ErbB4 captured by iTrap were diminished by addition of Iressa (50 μM) as a soluble competitor revealing the specificity of the iTrap reagent.

To determine whether Iressa directly bound to ErbB4, we used surface plasmon resonance (SPR) binding assays. We carried out SPR binding assays with the kinase domains of ErbB4 and EGFR using Iressa at concentrations ranging from 0 to 20 μM (Figure 6C,D). We found that Iressa bound both EGFR and ErbB4 with different affinities (Figure 6E,F), while the specific GSK-3β inhibitor, CHIR-99021, showed no interaction (Figure 6G,H). K_d's were determined from equilibrium binding measurements and by fitting these equilibrium measurements with a 1:1 interaction model using global parameters. K_d's for Iressa were determined to be approximately 30 and 150 nM for EGFR and ErbB4, respectively.

Finally, the effects of Iressa on the *in vitro* kinase activity of recombinant ErbB4 and EGFR were measured. Iressa was found to inhibit ErbB4 kinase domain activity *in vitro* with an $IC_{50} \approx 1$ μM (compared with 50 nM against EGFR), consistent with its EC_{50} for inhibition of Nrg1-induced neurite outgrowth (Figure 6I). Thus, in agreement with the iTrap affinity reagent studies and SPR binding assays, these biochemical findings provide support for the potential of direct interaction between Iressa and ErbB4 leading to a block of Nrg1-induced neuritogenesis.

Overall, our screen revealed that among the negative regulators of Nrg1−ErbB4 signaling, anilino-quinazolines are a rich source of inhibitors with diverse levels of efficacy and intra-ErbB family class specificity. Over the past decade, tremendous effort has been invested in ErbB receptor inhibition, especially targeting EGFR and ErbB2, because of their long-recognized role in cancer (*41*). As a result, a growing number of ErbB inhibitors have been identified. However, the specificity of these inhibitors has mostly been annotated by comparing EGFR and ErbB2, and no small molecules that are selective inhibitors of ErbB4 are currently available. Based on the close homology among ErbB family members in their kinase domain, several EGFR inhibitors, such as AG1478 and PD158780, have been considered as pan-ErbB inhibitors and used against ErbB4. Previously, these two inhibitors were shown to inhibit Nrg1-signaling and downstream biological consequences such as neurite outgrowth in hippocampal neurons (*42*), inhibition of NMDA receptor currents in pyramidal neurons from rodent prefrontal cortex (*43*), inhibition of long-term potentiation at Schaffer collateral-CA1 synapses in the hippocampus (*44*) and glutamatergic synapse maturation and plasticity (*45*). The identification of some of these compounds in our screen suggests that the cell-based imaging assay we developed may provide a surrogate system for identifying compounds that modulate Nrg1−ErbB4 regulated synaptic plasticity. However, dissecting ErbB4-specific inhibition from pan-ErbB inhibition poses a new challenge. We also noticed that, unlike Iressa or Traceva, PD158780 has an inhibitory effect on NGF-induced neurite outgrowth, which confounds the interpretation of results when this compound is used in physiological conditions where other neurotrophic factors might interfere. Thus, caution must be taken when these compounds are used because of potential off-target or indirect effects that might be attributed to inhibition of other hererodimerizing ErbB receptors instead of ErbB4 itself.

While this manuscript was in preparation, elegant studies by Krivosheya et al. (*40*) demonstrated that treatment of rat hippocampal neurons with soluble Nrg1 resulted in enhanced dendritic arborization through activation of the tyrosine kinase domain of ErbB4 and that RNAi-mediated silencing of ErbB4 decreased the number of primary neurites. These findings are consistent with our findings using RNAi toward ErbB4 in PC12 cells engineered to express this receptor and again provide evidence supporting the role of the kinase activity of ErbB4 in mediating neuritogenesis. However, our results differ in some aspects, as treatment of neurons with the PI3 kinase inhibitor LY294002, but

DOI: 10.1021/cn900046a | *ACS Chem. Neurosci.* (2010), *1*, 325–342

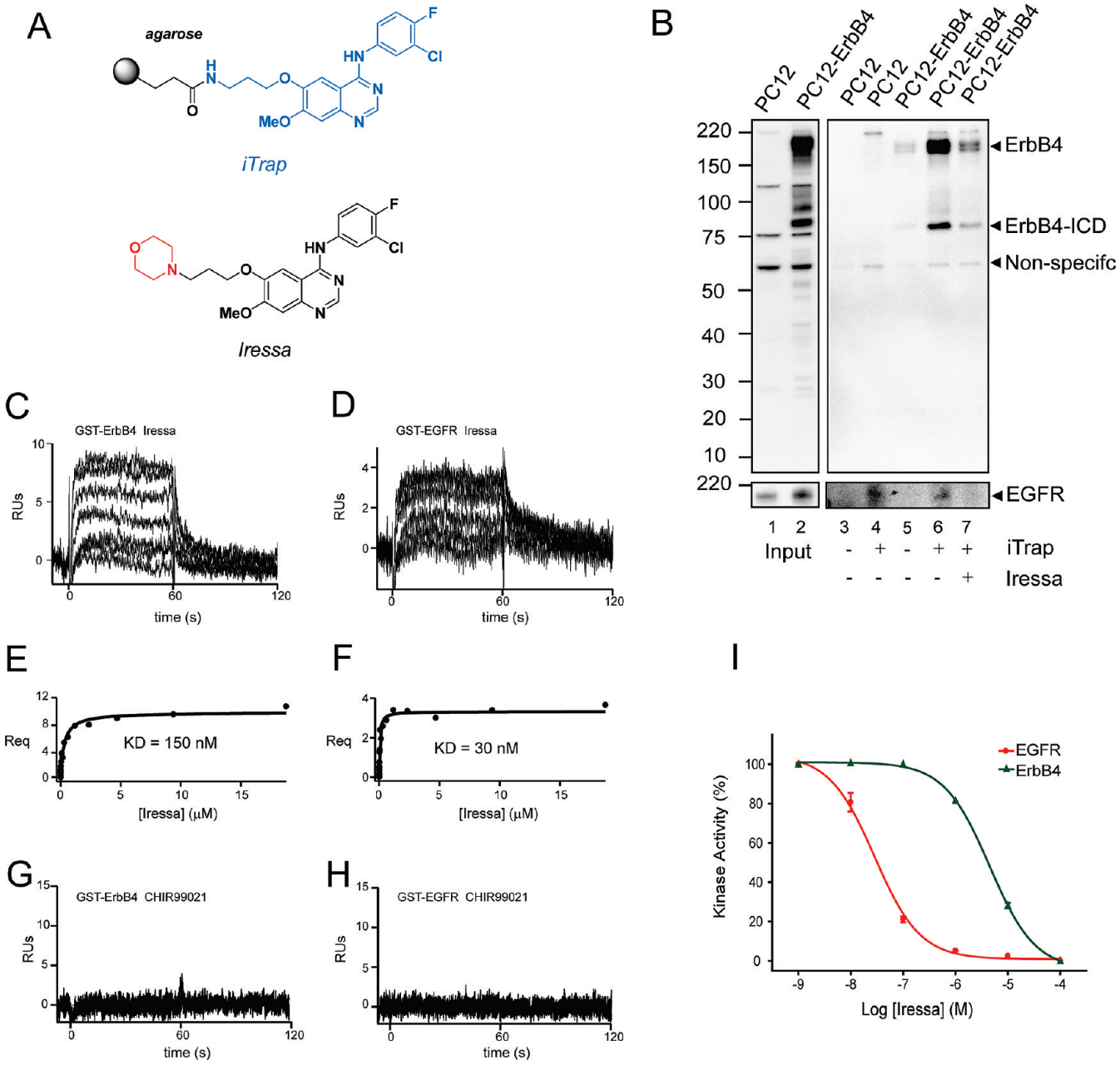

Figure 6. Characterization of Iressa's effect on Nrg1-induced signaling. (A) Schematic presentation of the agarose bead-conjugated Iressa (iTrap). (B) Whole cell extracts of PC12-GFP and PC12-ErbB4-GFP were premixed with or without 50 μM Iressa and subjected to affinity capture by control agarose beads (B) or agarose beads conjugated with Iressa (I). After four washes, the captured proteins were analyzed by Western blotting with antibodies against EGFR and ErbB4, respectively. A nonspecific band of 60 kDa detected by the anti-ErbB4 antibody was considered to ensure equal loading of samples. Surface plasmon resonance binding assays were carried out with GST-ErbB4 (C) and GST-EGFR (D) with Iressa. Sensorgrams from a representative assay are shown at Iressa concentrations of 4, 2, 0.092, 0.043, 0.001, and 0 μM. Equilibrium responses were measured and plotted versus Iressa concentration (in μM) for ErbB4 (E) and EGFR (F). The resulting theoretical fit to a 1:1 interaction model using global parameters is also plotted. K_d's for ErbB4 and EGFR were determined to be 150 and 30 nM respectively. Surface plasmon resonance binding assays were carried out with GST-ErbB4 (G) and GST-EGFR (H) with CHIR-99021. Sensorgrams from a representative assay are shown at CHIR-99021 concentrations of 4, 2, 0.092, 0.043, 0.001, and 0 μM. (I) Kinase activity of the kinase domain of recombinant EGFR and ErbB4 was determined in the presence of serially diluted Iressa relative to that of DMSO.

not the MAPK inhibitor PD980059, blocked neurite remodeling upon Nrg1 treatment. We speculate that these differences are due to differences in cell type and culture conditions.

Discovery of Small-Molecule Potentiators of Nrg1-ErbB4 Signaling

In addition to identifying inhibitors such as Iressa, our small-molecule screen also identified small molecules

DOI: 10.1021/cn900046a | ACS Chem. Neurosci. (2010), 1, 325–342

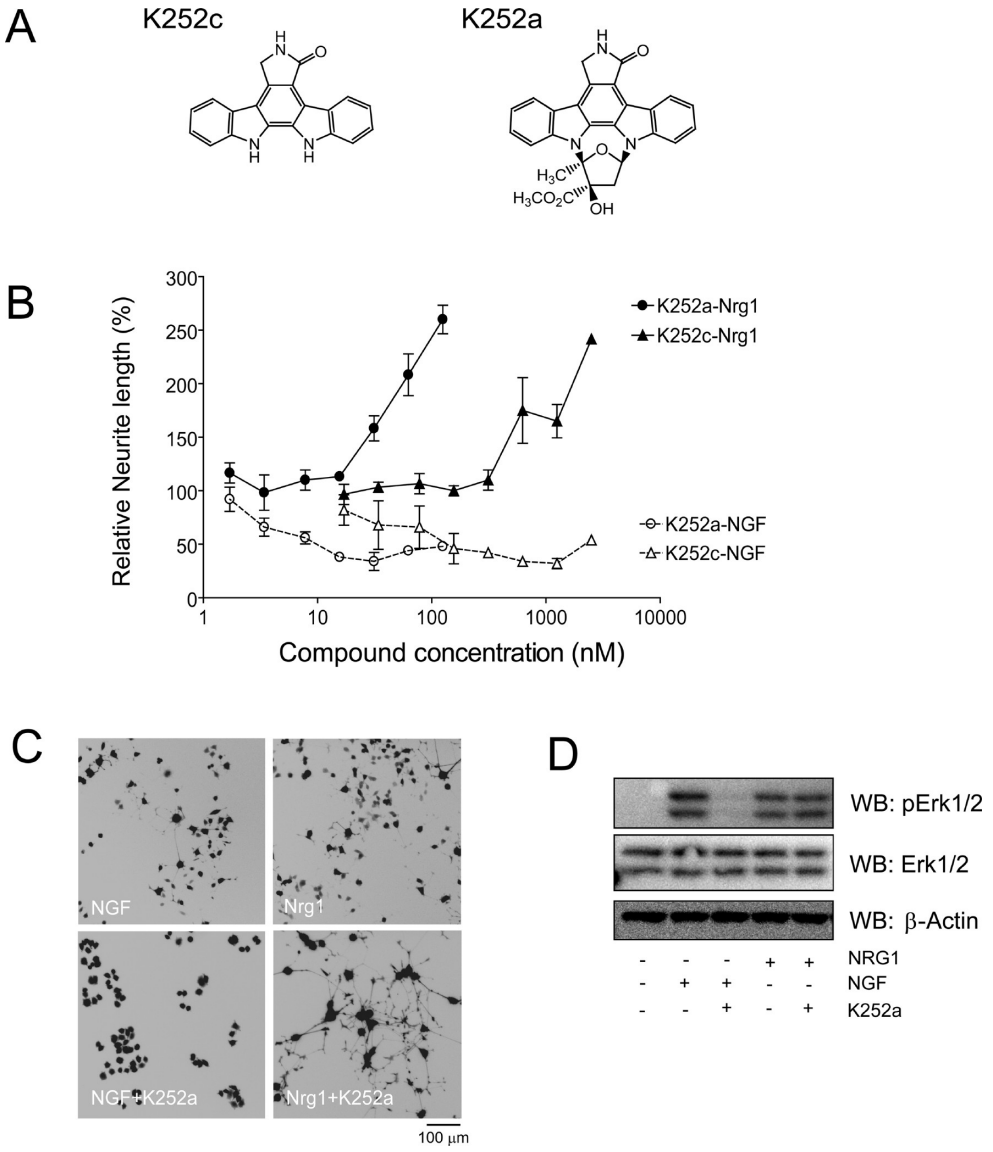

Figure 7. Characterization of indolocarbazoles that potentiate Nrg1-induced signaling. (A) Structures of K-252a and K-252c. (B) Cells were left untreated or were treated with K-252a (50 nM) for 30 min followed by treatment with 20 ng/mL of Nrg1 or NGF. Images were taken after 2 days. (C) Cells were treated with K-252a at various concentrations as indicated for 30 min followed by treatment with 20 ng/mL of Nrg1 or NGF. The mean neurite outgrowth per cell was measured after 2 days. (D) Cells were left untreated or were pretreated with DMSO or K-252a (50 nM) for 30 min followed by treatment with 20 ng/mL of NGF or Nrg1 and were lysed after 5 min. The levels of phospho-Erk1/2 were compared. Error bar represents SEM, $n = 4$.

that had no effect on NGF-induced neurite outgrowth but potentiated Nrg1-induced neurite outgrowth. One compound, the indolocarbazole, K-252c (Figure 7A), satisfied our selection criteria and furthermore had no effect on cell death or proliferation in the concentration range tested. Since K-252c is structurally similar to K-252a, a potent TrkA inhibitor that is widely used for inhibition of NGF-induced processes (e.g., refs *37*−*39*), we speculated that K-252a may also have effects on Nrg1−ErbB4 signaling. To test this hypothesis, we first treated the PC12-ErbB4-GFP cells with K-252a and NGF or Nrg1. As expected, K-252a completely inhibited NGF-induced neurite outgrowth at concentrations as low as 50 nM. In contrast, however, similar to K-252c, K-252a significantly potentiated Nrg1-induced neurite outgrowth at the same concentration that inhibited NGF-induced neurite outgrowth. Furthermore, both NGF inhibition and Nrg1 potentiation are dose-dependently modulated by K-252a (Figure 7B,C). Though we have yet to identify the specific target of K-252a that is responsible for mediating its effect on Nrg1−ErbB4 signaling, we and others have found that small modifications to the scaffold can afford remarkable selectivity (*46*, *47*). Functionally, the early Erk1/2 phosphorylation

DOI: 10.1021/cn900046a | *ACS Chem. Neurosci.* (2010), *1*, 325–342

in response to Nrg1 is not dramatically affected by K-252a treatment. On the other hand, NGF-induced Erk1/2 phosphorylation was diminished by K-252a (Figure 7D). These findings, and the potentiation of neuritogenesis phenotype, suggest that K-252a affects Nrg1 signaling in a manner distinct from its effects on Trk receptor mediated signaling.

Overall, the finding that Nrg1-induced neuritogenesis can be potentiated by both K-252a and NGF suggests that ErbB4 signaling in the brain can be enhanced by removing an inhibitory signal or by activating potentially intersecting or parallel signaling networks. It is possible that K-252a acts as a potent modulator of a downstream component shared by all the neurotrophic factors; however in the case of NGF signaling, its inhibitory effect on the TrkA receptor is dominant. K-252a has been shown previously to have a neuroprotective effect in several cell types through a mechanism reportedly due to inhibition of Trk family receptors (*48*, *49*). The detailed mechanism for K-252a's ability to potentiate Nrg1-induced signaling as observed here for the first time remains a challenge for future studies to address. While we speculate that the relevant target is a kinase, additional potential targets include other ATP-binding proteins such as ATPases involved in chromatin remodeling (e.g, SWI/SNF family) and cytoskeletal dynamics (e.g., myosin).

Conclusions

The ability of neurotrophic factors such as Nrg1 and NGF to regulate neuritogenesis, neuronal survival, differentiation, and aspects of synaptic plasticity is of fundamental importance to brain function and development. Yet our understanding of the underlying molecular mechanisms through which these factors operate is incomplete. A growing number of candidate neuropsychiatric disease risk genes and pathways, including Nrg1−ErbB4 characterized here, alter neurite formation (*22*). This suggests that *in vitro* cell culture systems that fulfill the needs of high-throughput screening (HTS), both with engineered systems and primary neurons or neural stem cells, can be used as surrogate systems to discover small-molecule probes that target signaling networks integral to the etiology and pathophysiology of severe mental illnesses.

The findings described here provide new insights to the regulation of neuritogenesis by the tyrosine kinase activity of ErbB4. They demonstrate the feasibility of using such a multidimensional, chemical-genetic approach for discovering probes of pathways implicated in neuropsychiatric disease. In our particular case, the ability to either potentiate or inhibit signaling with small-molecule probes will provide a means for testing the importance of Nrg1-ErbB4 signaling to psychiatric disease pathogenesis.

Collectively, our cellular and biochemical findings described above support the hypothesis that Iressa directly interacts with ErbB4 to inhibit Nrg1-induced neuritogenesis rather than through an indirect interaction with ErbB receptors that heterodimerize and transphosphorylate ErbB4. The use of the iTrap affinity reagents, SPR assays, and kinase assay highlight that Iressa is not selective within the ErbB family. From this latter finding, in combination with the RNAi-mediated gene silencing data, we conclude that the inhibition of EGFR signaling is neither detrimental nor beneficial for Nrg1-induced signaling involved in neurite outgrowth.

For the purpose of the present work, we focused on the feature of mean neurite outgrowth per cell because it was sensitive to the dose−response of Nrg1 and NGF treatment and correlated with many other cellular features. However, we recognize that further analysis of other features may lead to other modulators of Nrg1−ErbB4 signaling. In addition, expanded screening of libraries of known bioactives, purified natural products, FDA-approved drugs, and products of diversity-oriented synthesis using the system described here could also yield other useful chemical tools and improve in-depth understanding of Nrg1-mediated neurotrophic processes. An example is our recent description of a potent pyridine-containing molecule (Cpd-52), which potently (EC_{50} = 300 nM) inhibited Nrg1-induced neurite outgrowth (*50*). Further investigation of the electrophysiological and biochemical effects of the compounds identified in this study, along with target identification and more in depth exploration of the underlying structure−activity relationships, would provide important insight into the role of Nrg1 in regulating neural circuitry.

It will also be possible to extend these screening efforts to include other signaling pathways implicated in neuropsychiatric disorders, including brain-derived neurotrophic factor/TrkB. We anticipate that chemical genetics will provide a wealth of novel small-molecule probes for dissecting the neural circuitry implicated in neuropsychiatric diseases both in cells and *in vivo* in animal models. Iressa (gefitinib) and Tarceva (erlotinib) are under clinical investigation for the treatment of glioblastoma multiforme (GM). Since Iressa and Tarceva are relatively well tolerated, and can cross the blood−brain barrier (in patients with GM), these results suggest a translational paradigm in which the small molecules identified in our cell-based assays may provide a means to test the hypothesis that Nrg1−ErbB4 signaling is associated with abnormal behavioral states in animal models and potentially humans.

DOI: 10.1021/cn900046a | *ACS Chem. Neurosci.* (2010), *1*, 325–342

Methods

Materials

PC12 cells (subclone Neuroscreen-1) were obtained from Cellomics (Now ThermoFisher Scientific, Pittsburgh, PA). pcDNA3-ErbB4 (*51*) was kindly provided by Dr. Steven R. Vincent (University of British Columbia, Vancouver). Antibodies used were rabbit anti-ErbB4 c-18 and rabbit anti-phospho-ErbB4 (Santa Cruz Biotechnology, Santa Cruz, CA, nos. SC283 and SC33040), rabbit anti-phospho-p42/44 MAPK and rabbit anti-p42 MAPK (Cell Signaling Technology), and mouse anti-phosphotyrosine 4G10 (Upstate, Charlottesville, VA). The EGF domain of Nrg1β1 (corresponding to amino acid residues 176−246 of neuregulin-1β1), was expressed and purified from *Escherichia coli* (R&D Systems; no. 396-HB) and reconstituted in phosphate-buffered saline (PBS) with 0.1% bovine serum albumin as a nonspecific carrier and frozen in aliquots at −20 °C. Murine 2.5S nerve growth factor (Promega; G5141) was reconstituted in PBS 0.1% bovine serum albumin as a nonspecific carrier and frozen in aliquots at −20 °C. siRNA SmartPools for ErbB1, ErbB2, ErbB3, ErbB4, nontargeting, and DharmaFECT2 were purchased from Dharmacon, Chicago, IL (L080049, L090224, L088799, L080170, D001810, and T-2002-03, respectively).

Cell Culturing and Stable Cell Line Generation

PC12 cells were maintained in RPMI 1640 media (Gibco; 22400) containing 10% heat inactivated horse serum (Gibco; 26050), 5% heat inactivated fetal bovine serum (Gibco; 16140), and 1% penicillin/streptomycin (Gibco; 10378) referred to here as RPMI+. For PC12-ErbB4-GFP and PC12-GFP, 1% penicillin/streptomycin was replaced with 750 μg/mL gentamicin (Gibco; 15750). Cells were passaged at 80−90% confluency and incubated at 37 °C in 5% CO_2. Media was changed every 3 days. PC12 cells were cotransfected with pcDNA3-ErbB4-neomycin or pcDNA3-neomycin and pcDNA-GFP using FuGene 6 transfection reagent (Roche Diagnostics; 11814443). Cells that express the neomycin resistant gene were selected and maintained in same culture media with substitution of 750 μg/mL G418. After 2 weeks of G418 selection, cells were further selected by fluorescence-activated cell sorting (FACS) using a MoFlo Cell Sorter (Dako, Denmark) of the top 5% most strongly GFP expressing cells. The expression of GFP in the resulting cell populations, PC12-ErbB4-GFP and PC12-GFP, was observed to be stable for at least 50 passages.

Immunoprecipitation and Western Blotting

Cells were lysed with RIPA buffer (Pierce Technology, Rockford, IL; 89901) containing 1 tablet/10 mL protease inhibitor cocktail Complete Mini (Roche Applied Science; 11836153). For phosphoprotein analysis, Halt Phosphatase Inhibitor Cocktail (Pierce Technology; 78415) was also included. Cell lysates were cleared by centrifugation at 15 000 rpm for 30 min at 4 °C followed by addition of LDS sample buffer (Invitrogen; NP008) for direct analysis or were immunoprecipitated with specific primary antibodies and Protein A/G agarose (Pierce Technology 20421) following the manufacturer's protocol. Samples were separated using a 4−12% gradient gel (Invitrogen) and SDS−PAGE and transferred to a polyvinylidene difluoride (PVDF; Schleicher & Schnell 10413096) membrane in 25 mM Tris, 192 mM glycine, and 20% methanol. The membrane was probed with specific primary antibodies according to specified recipes provided by their venders and then horseradish peroxidase-conjugated secondary antibody to mouse or rabbit IgG (GE Healthcare, Piscataway, NJ; NA934V and NA931V). Target protein bands were detected with SuperSignal West Femto Max Sensitivity Substrate (Pierce Technology; 34095).

siRNA Knockdown of ErbB Receptors

Cells were typically seeded at a density of 4000 cells/cm^2 and incubated for 12 h. siRNAs were prepared as 1 μM solution in serum-free medium and DharmaFECT2 was diluted 2:100 (v/v) with serum-free medium. Both solutions were incubated at room temperature for 5 min before mixing thoroughly and incubating for additional 20 min. The transfection mix was then added to cell culture at 1:5 (v/v). The cells were incubated for 24 h at 37 °C in 5% CO_2 and treated with neurotrophic factors or directly lysed for Western blot analysis.

Cell Imaging and Neurite Measurements

Cells were seeded in black, clear bottom, tissue culture-treated 96-well (Corning; 3904) or 384-well (Corning; 3712) plates at typical density of 4000 cells/cm^2 corresponding to approximately 1200 cells per well of a 96-well plate in 100 μL of media and 300 cells per well of a 384-well plate in 40 μL of RPMI medium. Even distribution was achieved by a quick centrifugation at 500 rpm using a tabletop centrifuge (Sorvall, LegendRT) and multiwell plate adaptors shortly after seeding. Cells were then incubated for 12 h followed by treatment with growth factors or compounds as indicated. At specified time points, fluorescent images were taken using an ImageXpress 5000A or ImageXpress Micro automated microscopy (Molecular Devices) either manually or laser-based, autofocus with a Nikon 4× objective (ELWD S Fluor/0.20 NA) and an image acquisition time of 150 ms or as specified. Transmitted light images were taken using an ImageXpress Micro (Molecular Devices) with an attached transmitted light device with a Nikon 4× objective (ELWD S Fluor/0.20 NA). Neurite detection and analysis were performed with MetaXpress (Molecular Devices) using the "Neurite Detection" analysis module. Cell bodies were specified as pixel blocks of maximum width 40 μm, minimum area 200 μm^2, and pixel intensities 1000 units above local background. Neurites were specified as linear objects with maximum width 3 μm and pixel intensities 500 units above the local background of the object being measured. Fluorescent images shown were imported as tagged image file format (TIFF) files into Adobe Photoshop (San Jose, CA) and in specified cases overlaid with transmitted light images that were processed in the same manner. After more than 4 days of incubation, significant cell detachment, cell clumping, and decreased GFP signal were observed and eventually caused aberrant detection of neurites. Although a longer exposure is potentially achievable by changing the cellular medium, we concluded that our automated neurite detection methods with up to 4 days incubation can reliably report the effects of Nrg1 and NGF on neurite induction and is sufficient to study quantitatively the kinetics of neurite outgrowth.

HTS of Morphological Features

Cells were seeded into black, clear bottom, tissue culture-treated 96-well (Corning; 3904) or 384-well (Corning; 3712)

DOI: 10.1021/cn900046a | ACS Chem. Neurosci. (2010), 1, 325–342

plates at typical density of 4000 cells/cm^2 corresponding to approximately 1200 cells per well of a 96-well plate in 100 μL of RPMI media and 300 cells per well of a 384-well plate in 40 μL of RPMI media. Even distribution was achieved by a quick centrifugation at 500 rpm using a tabletop centrifuge (Sorvall, LegendRT) and multiwell plate adaptors shortly after seeding. Cells were then incubated for 12 h to allow attachment. A total of 400 compounds, along with a total of 752 DMSO controls, were pin-transferred into wells of 384-well plates containing PC12-ErbB4-GFP cells prior to treatment of Nrg1 or NGF. After pinning compounds, either Nrg1 (20 ng/mL) or NGF (20 ng/mL) was added robotically to each well that received compound. At time points as specified, images were taken using ImageXpress 5000A (Molecular Devices) or ImageXpress Micro (Molecular Devices) automated microscopy systems using either manual or laser-based autofocus with a Nikon 4× objective (ELWD S Fluor/0.20 NA) and an image acquisition time of 150 ms using a xenon light source and 483/536 nm filter sets for measuring GFP fluorescence. Transmitted light images were taken using an ImageXpress Micro (Molecular Devices) with an attached transmitted light device with a Nikon 4× objective (ELWD S Fluor/0.20 NA). Neurite detection and analysis were performed with MetaXpress (Molecular Devices) using the "Neurite Detection" analysis module. Cell bodies were specified as pixel blocks of maximum width 40 μm, minimum area 200 μm^2, and pixel intensities 1000 units above local background. Neurites were specified as linear objects with maximum width 3 μm and pixel intensities 500 units above the local background of the object being measured. Cell morphological features measured using MetaXpress software included: "% Cells Significant Growth" (the percentage of cells that have neurites of at least 10 μm in length), "Number of Cells" (the total cell count in the well of 384 well plate), "Total Outgrowth" (the total length of neurite within the well in micrometers), "Mean Outgrowth Per Cell" (the average total length of neurite per cell in micrometers), "Mean Processes Per Cell" (the average number of neurites per cell), "Normalized Mean Neurite Length" (the average length of neurite per cell in micrometers normalized to the values of DMSO treated wells), "Mean Branches Per Cell" (the average number of neurite branches per cell), "Mean Cell Body Area" (the average size of the cell in square micrometers). Processed screening data were visualized using Spotfire DecisionSite software (Somerville, MA) and in Microsoft Excel (Seattle, WA).

Compound Library and Screening Method

A custom library of 400 known bioactive compounds was assembled from commercial sources (Calbiochem, Sigma, Biomol, and Tocris) and stored in DMSO at −80 °C in custom dryboxes (see Supplementary Tables 1 and 2, Supporting Information, for a full list of compounds screened in the two conditions). For primary screening, compounds were robotically pin-transferred from 10 mM stocks in DMSO to a final concentration of ∼10 μM using a CyBio CyBi-Well vario equipped with a 50 nL pin head. Follow-up characterization was performed on reordered stocks or compounds purified from expired pharmaceutical-grade tablets (Iressa and Tarceva).

Surface Plasmon Resonance Assays

The EGFR/ErbB4 surface plasmon resonance assays were conducted on a Biacore T100 instrument using Biacore CM5 sensor chips. Ethanolamine, EDC, NHS, and P-20 surfactant were all obtained from GE Lifesciences. An anti-GST antibody (GST capture kit, GE LifeSciences) was directly immobilized through primary amines using standard EDC/NHS chemistry according to the manufacturer's instructions. Either GST alone or GST-ErbB4 (Cell Signaling) or GST-EGFR (Millipore) was captured to generate the ErbB4 or EGFR sensor chips, respectively. GST-fusion proteins were thawed immediately before use and kept at 4 °C during sample preparation. Binding assays were performed at 25 °C. The EGFR/ErbB4 assays were carried out in 1× PBS, 2% DMSO, 0.005% P-20 surfactant (PBS−P20). Compounds were injected at a flow rate of 30 μL/min into the flow cell for 60 s followed by 60 s of buffer without compound. Iressa and CHIR-99021 were stored in 100% DMSO and diluted into PBS−P20 with 2% DMSO for binding assays. CHIR-99021 activity was verified by binding to GST-GSK3β (BPS Biosciences) under identical conditions. Sensorgram data was analyzed using both Scrubber 2 software (BioLogic Software Pty) and Biacore T100 Evaluation software. Data was GST-reference subtracted and corrected for protein capture, DMSO concentration, and analyte molecular weight. K_d values were determined from steady-state binding values (R_{eq}) measured at 56 s of a 60 s injection and averaged over a 5 s window. Steady-state binding values were plotted against concentration values and fit using a model assuming 1:1 analyte to ligand binding.

Affinity-Based Capture of ErbB4 with iTrap

See Supporting Information for detailed synthetic method and characterization of the iTrap affinity reagent. PC12-ErbB4-GFP cells were lysed with a modified RIPA buffer (50 mM Tris-HCl, pH 7.4, 1% NP40, 250 mM NaCl, 1 mM EDTA, 1 mM NaF, 1 mM Na_3VO_4, supplemented with an EDTA-free protease inhibitor cocktail) at 4 °C for 10 min, and the cell lysate was cleared by centrifugation. The cleared lysate (0.4 mL) was tumbled with Iressa or DMSO at indicated concentration at 4 °C for 30 min before addition of the iTrap resin (10 μL). The resulting mixture was tumbled at 4 °C for 12 h. The suspension was centrifuged, and the supernatant was discarded. The resin was washed with the above modified RIPA buffer (1 mL) for four times. After the final wash, the supernatant was removed, and SDS sample buffer (20 μL) was added to the resin. The affinity purified proteins were heat denatured and separated by SDS−PAGE. Western immunoblotting experiment was then performed using anti-ErbB4 antibody (BD Biosciences, Cat. No. 610808) following the manufacturer's protocol.

Supporting Information Available

Description of instruments and materials, figures showing synergistic effect of cotreatment of PC12-ErbB4-GFP cells with NGF and Nrg1, the effect of additional 4-anilinoquinazolines on Nrg1 and NGF-induced neuritogenesis, graphical representation of two-dimensional correlation map between eight cellular features in the Nrg1 and NGF

DOI: 10.1021/cn900046a | ACS Chem. Neurosci. (2010), 1, 325–342

high-content imaging screens, and comparison of relationships among eight cellular features from high-content imaging screen of Nrg1-induced neuritogenesis, and tables showing Nrg1 and NGF data sets from complete screen, Nrg1 and NGF data sets from DMSO controls only, Nrg1 and NGF data sets from compounds only, Nrg1 and NGF descriptive statistics and correlation analysis of data sets from compounds only. This material is available free of charge via the Internet at http://pubs.acs.org.

Author Information

Corresponding Author

* Mailing address: Department of Neurology, Harvard Medical School Stanley Center for Psychiatric Research Broad Institute of Harvard and MIT Center for Human Genetic Research Massachusetts General Hospital 185 Cambridge Street, 5.412 (office), Boston, MA 02114. Tel: (617) 643-3201. Fax: (617) 726-6982; E-mail: haggarty@chgr.mgh.harvard.edu.

Author Contributions

Letian Kuai, Xiang Wang, and Jon M. Madison performed the experimental work and data analysis described herein. Stuart L. Schreiber, Edward M. Scolnick, and Stephen J. Haggarty provided guidance and advice. The manuscript was written through contributions of all authors. All authors have given approval to the final version of the manuscript.

Funding Sources

L.K. and S.J.H were supported by funds from the Stanley Medical Research Institute and the Broad Institute SPARC program. S.J.H. was also supported in part by Grants 1R21MH076146-01 (NIMH) and 1R21MH087896-01 (NIMH). The National Cancer Institute's Initiative for Chemical Genetics (Contract No. N01-CO-12400) provided support for the Broad Chemical Biology Platform.

Notes

The authors report no conflicts of interest.

Acknowledgment

We thank Pamela Sklar, Tracey L. Petryshen, Martha Constatine-Paton, Steve A. Carr, and Shao-En Ong for helpful comments throughout this work. Steven R. Vincent (University of British Columbia, Vancouver) is thanked for providing the pcDNA-ErbB4 cDNA clone. Ralph Mazitschek and James E. Bradner are thanked for providing Iressa and Tarceva. Daniel M. Fass is thanked for helping generate cell lines. We wish to thank the National Cancer Institute's Initiative for Chemical Genetics (contract no. N01-CO-12400), who provided support for this publication, and the Chemical Biology Platform of the Broad Institute of Harvard and MIT for their assistance in this work. The content of this publication does not necessarily reflect the views or policies of the Department of Health and Human Service, nor does mention of trade names, commercial products, or organizations imply endorsement by the U.S. Government.

Abbreviations

EDC, (1-ethyl-3-[3-dimethylaminopropyl]carbodiimide hydrochloride; EGFR, epidermal growth factor receptor; ErbB4, v-erb-a erythroblastic leukemia viral oncogene homologue 4; GFP, green fluorescent protein; MAPK, mitogen-activated protein kinase; NGF, nerve growth factor; NHS, *N*-hydroxysuccinimide; Nrg1, neuregulin-1; PI3K, phosphotidylinositol-3 kinase.

References

1. Smukste, I., and Stockwell, B. R. (2005) Advances in chemical genetics. *Annu. Rev. Genomics Hum. Genet. 6*, 261–286.

2. Harrison, P. J., and Law, A. J. (2006) Neuregulin 1 and schizophrenia: Genetics, gene expression, and neurobiology. *Biol. Psychiatry 60*, 132–140.

3. Ross, C. A., Margolis, R. L., Reading, S. A., Pletnikov, M., and Coyle, J. T. (2006) Neurobiology of schizophrenia. *Neuron 52*, 139–153.

4. Stefansson, H., Sigurdsson, E., Steinthorsdottir, V., Bjornsdottir, S., Sigmundsson, T., Ghosh, S., Brynjolfsson, J., Gunnarsdottir, S., Ivarsson, O., Chou, T. T., Hjaltason, O., Birgisdottir, B., Jonsson, H., Gudnadottir, V. G., Gudmundsdottir, E., Bjornsson, A., Ingvarsson, B., Ingason, A., Sigfusson, S., Hardardottir, H., Harvey, R. P., Lai, D., Zhou, M., Brunner, D., Mutel, V., Gonzalo, A., Lemke, G., Sainz, J., Johannesson, G., Andresson, T., Gudbjartsson, D., Manolescu, A., Frigge, M. L., Gurney, M. E., Kong, A., Gulcher, J. R., Petursson, H., and Stefansson, K. (2002) Neuregulin 1 and susceptibility to schizophrenia. *Am. J. Hum. Genet. 71*, 877–892.

5. Benzel, I., Bansal, A., Browning, B. L., Galwey, N. W., Maycox, P. R., McGinnis, R., Smart, D., St Clair, D., Yates, P., and Purvis, I. (2007) Interactions among genes in the ErbB-Neuregulin signalling network are associated with increased susceptibility to schizophrenia. *Behav. Brain Funct. 3*, 31.

6. Norton, N., Moskvina, V., Morris, D. W., Bray, N. J., Zammit, S., Williams, N. M., Williams, H. J., Preece, A. C., Dwyer, S., Wilkinson, J. C., Spurlock, G., Kirov, G., Buckland, P., Waddington, J. L., Gill, M., Corvin, A. P., Owen, M. J., and O'Donovan, M. C. (2006) Evidence that interaction between neuregulin 1 and its receptor erbB4 increases susceptibility to schizophrenia. *Am. J. Med. Genet., Part B 141*, 96–101.

7. Silberberg, G., Darvasi, A., Pinkas-Kramarski, R., and Navon, R. (2006) The involvement of ErbB4 with schizophrenia: Association and expression studies. *Am. J. Med. Genet., Part B 141*, 142–148.

8. Law, A. J., Kleinman, J. E., Weinberger, D. R., and Weickert, C. S. (2007) Disease-associated intronic variants in the ErbB4 gene are related to altered ErbB4 splice-variant expression in the brain in schizophrenia. *Hum. Mol. Genet. 16*, 129–141.

9. Nicodemus, K. K., Luna, A., Vakkalanka, R., Goldberg, T., Egan, M., Straub, R. E., and Weinberger, D. R. (2006) Further evidence for association between ErbB4 and schizophrenia and influence on cognitive intermediate phenotypes in healthy controls. *Mol. Psychiatry 11*, 1062–1065.

10. Law, A. J., Lipska, B. K., Weickert, C. S., Hyde, T. M., Straub, R. E., Hashimoto, R., Harrison, P. J., Kleinman,

J. E., and Weinberger, D. R. (2006) Neuregulin 1 transcripts are differentially expressed in schizophrenia and regulated by 5′ SNPs associated with the disease. *Proc. Natl. Acad. Sci. U.S.A. 103*, 6747–6752.

11. Petryshen, T. L., Middleton, F. A., Kirby, A., Aldinger, K. A., Purcell, S., Tahl, A. R., Morley, C. P., McGann, L., Gentile, K. L., Rockwell, G. N., Medeiros, H. M., Carvalho, C., Macedo, A., Dourado, A., Valente, J., Ferreira, C. P., Patterson, N. J., Azevedo, M. H., Daly, M. J., Pato, C. N., Pato, M. T., and Sklar, P. (2005) Support for involvement of neuregulin 1 in schizophrenia pathophysiology, *Mol. Psychiatry 10*, 366−374, 328.

12. Corfas, G., Roy, K., and Buxbaum, J. D. (2004) Neuregulin 1-erbB signaling and the molecular/cellular basis of schizophrenia. *Nat. Neurosci. 7*, 575–580.

13. Mei, L., and Xiong, W. C. (2008) Neuregulin 1 in neural development, synaptic plasticity and schizophrenia. *Nat. Rev. Neurosci. 9*, 437–452.

14. Chong, V. Z., Thompson, M., Beltaifa, S., Webster, M. J., Law, A. J., and Weickert, C. S. (2008) Elevated neuregulin-1 and ErbB4 protein in the prefrontal cortex of schizophrenic patients. *Schizophrenia Res. 100*, 270–280.

15. Hahn, C. G., Wang, H. Y., Cho, D. S., Talbot, K., Gur, R. E., Berrettini, W. H., Bakshi, K., Kamins, J., Borgmann-Winter, K. E., Siegel, S. J., Gallop, R. J., and Arnold, S. E. (2006) Altered neuregulin 1-erbB4 signaling contributes to NMDA receptor hypofunction in schizophrenia. *Nat. Med. 12*, 824–828.

16. Falls, D. L. (2003) Neuregulins and the neuromuscular system: 10 years of answers and questions. *J. Neurocytol. 32*, 619–647.

17. Elenius, K., Choi, C. J., Paul, S., Santiestevan, E., Nishi, E., and Klagsbrun, M. (1999) Characterization of a naturally occurring ErbB4 isoform that does not bind or activate phosphatidyl inositol 3-kinase. *Oncogene 18*, 2607–2615.

18. Elenius, K., Corfas, G., Paul, S., Choi, C. J., Rio, C., Plowman, G. D., and Klagsbrun, M. (1997) A novel juxtamembrane domain isoform of HER4/ErbB4. Isoform-specific tissue distribution and differential processing in response to phorbol ester. *J. Biol. Chem. 272*, 26761–26768.

19. Carpenter, G. (2003) ErbB-4: Mechanism of action and biology. *Exp. Cell Res. 284*, 66–77.

20. Tao, R. H., and Maruyama, I. N. (2008) All EGF(ErbB) receptors have preformed homo- and heterodimeric structures in living cells. *J. Cell Sci. 121*, 3207–3217.

21. Linggi, B., and Carpenter, G. (2006) ErbB receptors: New insights on mechanisms and biology. *Trends Cell Biol. 16*, 649–656.

22. Bellon, A. (2007) New genes associated with schizophrenia in neurite formation: A review of cell culture experiments. *Mol. Psychiatry 12*, 620–629.

23. Greene, L. A., and Tischler, A. S. (1976) Establishment of a noradrenergic clonal line of rat adrenal pheochromocytoma cells which respond to nerve growth factor. *Proc. Natl. Acad. Sci. U.S.A. 73*, 2424–2428.

24. Vaskovsky, A., Lupowitz, Z., Erlich, S., and Pinkas-Kramarski, R. (2000) ErbB-4 activation promotes neurite outgrowth in PC12 cells. *J. Neurochem. 74*, 979–987.

25. Sardi, S. P., Murtie, J., Koirala, S., Patten, B. A., and Corfas, G. (2006) Presenilin-dependent ErbB4 nuclear signaling regulates the timing of astrogenesis in the developing brain. *Cell 127*, 185–197.

26. Vaghefi, H., and Neet, K. E. (2004) Deacetylation of p53 after nerve growth factor treatment in PC12 cells as a post-translational modification mechanism of neurotrophin-induced tumor suppressor activation. *Oncogene 23*, 8078–8087.

27. Rankin, S. L., Guy, C. S., and Mearow, K. M. (2005) TrkA NGF receptor plays a role in the modulation of p75NTR expression. *Neurosci. Lett. 383*, 305–310.

28. Sergina, N. V., Rausch, M., Wang, D., Blair, J., Hann, B., Shokat, K. M., and Moasser, M. M. (2007) Escape from HER-family tyrosine kinase inhibitor therapy by the kinase-inactive HER3. *Nature 445*, 437–441.

29. Pang, L., Sawada, T., Decker, S. J., and Saltiel, A. R. (1995) Inhibition of MAP kinase kinase blocks the differentiation of PC-12 cells induced by nerve growth factor. *J. Biol. Chem. 270*, 13585–13588.

30. Gambarotta, G., Garzotto, D., Destro, E., Mautino, B., Giampietro, C., Cutrupi, S., Dati, C., Cattaneo, E., Fasolo, A., and Perroteau, I. (2004) ErbB4 expression in neural progenitor cells (ST14A) is necessary to mediate neuregulin-1beta1-induced migration. *J. Biol. Chem. 279*, 48808–48816.

31. Kim, Y., Seger, R., Suresh Babu, C. V., Hwang, S. Y., and Yoo, Y. S. (2004) A positive role of the PI3-K/Akt signaling pathway in PC12 cell differentiation. *Mol. Cells 18*, 353–359.

32. Ghosh, S., Jennissen, J. D., Liu, X. P., and Uckun, F. M. (2001) 4-[3-Bromo-4-hydroxyphenyl)amino]-6,7-dimethoxy-quinazolin-1-ium chloride methanol solvate and 4-[(3-hydroxyphenyl)amino]-6,7-dimethoxy-1-quinazolinium chloride. *Acta Crystallogr. C57*, 76–78.

33. Discafani, C. M., Carroll, M. L., Floyd, M. B., Jr., Hollander, I. J., Husain, Z., Johnson, B. D., Kitchen, D., May, M. K., Malo, M. S., Minnick, A. A., Jr., Nilakantan, R., Shen, R., Wang, Y. F., Wissner, A., and Greenberger, L. M. (1999) Irreversible inhibition of epidermal growth factor receptor tyrosine kinase with in vivo activity by N-[4-[(3-bromophenyl)amino]-6-quinazolinyl]-2-butynamide (CL-387,785). *Biochem. Pharmacol. 57*, 917–925.

34. Han, Y., Caday, C. G., Nanda, A., Cavenee, W. K., and Huang, H. J. (1996) Tyrphostin AG 1478 preferentially inhibits human glioma cells expressing truncated rather than wild-type epidermal growth factor receptors. *Cancer Res. 56*, 3859–3861.

35. Jani, J. P., Finn, R. S., Campbell, M., Coleman, K. G., Connell, R. D., Currier, N., Emerson, E. O., Floyd, E., Harriman, S., Kath, J. C., Morris, J., Moyer, J. D., Pustilnik, L. R., Rafidi, K., Ralston, S., Rossi, A. M., Steyn, S. J., Wagner, L., Winter, S. M., and Bhattacharya, S. K. (2007) Discovery and pharmacologic characterization of CP-724,714, a selective ErbB2 tyrosine kinase inhibitor. *Cancer Res. 67*, 9887–9893.

36. Wakeling, A. E., Guy, S. P., Woodburn, J. R., Ashton, S. E., Curry, B. J., Barker, A. J., and Gibson, K. H. (2002) ZD1839 (Iressa): An orally active inhibitor of epidermal

DOI: 10.1021/cn900046a | *ACS Chem. Neurosci.* (2010), *1*, 325–342

growth factor signaling with potential for cancer therapy. *Cancer Res. 62*, 5749–5754.

37. Koizumi, S., Contreras, M. L., Matsuda, Y., Hama, T., Lazarovici, P., and Guroff, G. (1988) K-252a: A specific inhibitor of the action of nerve growth factor on PC 12 cells. *J. Neurosci. 8*, 715–721.

38. Doherty, P., and Walsh, F. S. (1989) K-252a specifically inhibits the survival and morphological differentiation of NGF-dependent neurons in primary cultures of human dorsal root ganglia. *Neurosci. Lett. 96*, 1–6.

39. Perez-Pinera, P., Hernandez, T., Garcia-Suarez, O., de Carlos, F., Germana, A., Del Valle, M., Astudillo, A., and Vega, J. A. (2006) The Trk tyrosine kinase inhibitor K252a regulates growth of lung adenocarcinomas. *Mol. Cell. Biochem. 295*, 19–26.

40. Krivosheya, D., Tapia, L., Levinson, J. N., Huang, K., Kang, Y., Hines, R., Ting, A. K., Craig, A. M., Mei, L., Bamji, S. X., and El-Husseini, A. (2008) ErbB4-neuregulin signaling modulates synapse development and dendritic arborization through distinct mechanisms. *J. Biol. Chem. 283*, 32944–32956.

41. Zhang, H., Berezov, A., Wang, Q., Zhang, G., Drebin, J., Murali, R., and Greene, M. I. (2007) ErbB receptors: From oncogenes to targeted cancer therapies. *J. Clin. Invest. 117*, 2051–2058.

42. Gerecke, K. M., Wyss, J. M., and Carroll, S. L. (2004) Neuregulin-1beta induces neurite extension and arborization in cultured hippocampal neurons. *Mol. Cell. Neurosci. 27*, 379–393.

43. Gu, Z., Jiang, Q., Fu, A. K., Ip, N. Y., and Yan, Z. (2005) Regulation of NMDA receptors by neuregulin signaling in prefrontal cortex. *J. Neurosci. 25*, 4974–4984.

44. Kwon, O. B., Longart, M., Vullhorst, D., Hoffman, D. A., and Buonanno, A. (2005) Neuregulin-1 reverses long-term potentiation at CA1 hippocampal synapses. *J. Neurosci. 25*, 9378–9383.

45. Li, B., Woo, R. S., Mei, L., and Malinow, R. (2007) The neuregulin-1 receptor erbB4 controls glutamatergic synapse maturation and plasticity. *Neuron 54*, 583–597.

46. Bishop, A. C., Ubersax, J. A., Petsch, D. T., Matheos, D. P., Gray, N. S., Blethrow, J., Shimizu, E., Tsien, J. Z., Schultz, P. G., Rose, M. D., Wood, J. L., Morgan, D. O., and Shokat, K. M. (2000) A chemical switch for inhibitor-sensitive alleles of any protein kinase. *Nature 407*, 395–401.

47. Tamaki, K., Shotwell, J. B., White, R. D., Drutu, I., Petsch, D. T., Nheu, T. V., He, H., Hirokawa, Y., Maruta, H., and Wood, J. L. (2001) Efficient syntheses of novel C2′-alkylated (±)-K252a analogues. *Org. Lett. 3*, 1689–1692.

48. Roux, P. P., Dorval, G., Boudreau, M., Angers-Loustau, A., Morris, S. J., Makkerh, J., and Barker, P. A. (2002) K252a and CEP1347 are neuroprotective compounds that inhibit mixed-lineage kinase-3 and induce activation of Akt and ERK. *J. Biol. Chem. 277*, 49473–49480.

49. Berg, M. M., Sternberg, D. W., Parada, L. F., and Chao, M. V. (1992) K-252a inhibits nerve growth factor-induced trk proto-oncogene tyrosine phosphorylation and kinase activity. *J. Biol. Chem. 267*, 13–16.

50. Gray, B. L., Wang, X., Brown, W. C., Kuai, L., and Schreiber, S. L. (2008) Diversity synthesis of complex pyridines yields a probe of a neurotrophic signaling pathway. *Org. Lett. 10*, 2621–2624.

51. Fleisig, H., El-Din El-Husseini, A., and Vincent, S. R. (2004) Regulation of ErbB4 phosphorylation and cleavage by a novel histidine acid phosphatase. *Neuroscience 127*, 91–100.

DOI: 10.1021/cn900046a | *ACS Chem. Neurosci.* (2010), *1*, 325–342